# Interference Drag of Multiple Pressure Cushions

**Ronald W. Yeung¶, Hui Wan, and Jae-Moon Lew***
Department of Mechanical Engineering
University of California at Berkeley, Berkeley, CA 94720-1740, USA
¶Correspondence author. E-mails: *rwyeung@berkeley.edu*, *wanh@berkeley.edu*, & *jmlew@cnu.ac.kr*

## 1 Background

Faster speed, yet lower power consumption, has often been the design objective of high-performance marine vehicles such as hovercrafts, Surface-Effect Ships (SES), among others. Lower power consumption also means less carbon-dioxide emission, an issue of great environmental concern. The concept of a multi-hull system offers favorable possibility of powering reduction in steady motion. Configuration arrangement of component hulls is therefore an important design issue to address.

The problems of steady forward-motion of multi-hulls and SES (hulls with a pressure cushion) were analyzed in Yeung et al. [1], and Yeung & Wan [2], respectively. Therein, linearized theory was used to obtain the interference wave resistance, which can be either positive or negative, increasing or reducing the powering for a given speed. Results for a single pressure cushion are quite well known (see, e.g., Wehausen & Laitone [3], Newman & Poole [4], and Doctors & Sharma [5]). The possibility of shaping the pressure function within a cushion was considered in the interesting work of Tuck et al. [6]. However, the effects of combining multiple numbers of cushions, perhaps even of dis-similar shapes, have yet to be thoroughly explored. This paper addresses the multiple pressure-cushion problem in the same vein as [1] & [2], with the aim of obtaining the necessary interference expressions for rapid evaluation of the behavior of a pressure collection. Given that there have been reports [7] on the use of multiple cushions to successfully improve the rides and maneuverability of SES and other cushioned crafts, developing a methodology to assess the powering performance of multi-cushions is desirable.

## 2 Resistance of a Translating Pressure Cushion

Within the framework of linear theory, the generalized steady wave resistance problem can be summarized

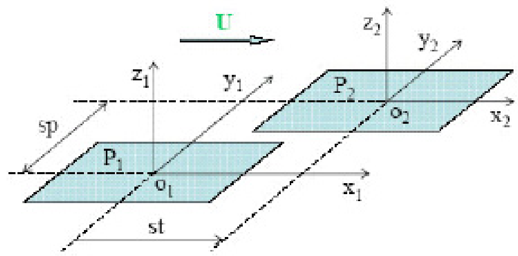


Figure 1: *Coordinate systems: shown for two pressure cushions with separation and stagger.*

as finding a velocity potential $\phi(x, y, z)$ that satisfies Laplace's equation, but is subject to the free-surface boundary condition:

$$k_0\phi_z(x, y, 0)+\phi_{xx}(x, y, 0)=P_x(x, y)/\rho U \qquad (1)$$

where $k_0 = g/U^2$ and $U$ is the forward speed in direction $x$ (Fig. 1) and $\rho$ the water density. Here, $P(x, y)$ is the applied (cushion) pressure, which vanishes except in the planform regions $S_P$. Conditions of decaying disturbances as $z\to-\infty$ and the absence of upstream waves ($x\to\infty$) are also to be observed. We note also that the linearized fluid pressure $p$ and the longitudinal free-surface slope $\zeta_x$ are given by:

$$p(x, y, z) - P(x, y) = -\rho U\phi_x + \rho gz, \qquad (2)$$

$$g\zeta_x(x, y) = U\phi_{xx}(x, y, 0) - P_x/\rho. \qquad (3)$$

The velocity potential $\phi_P(x, y, z)$ can be given in terms of derivative of the Green function $G$ as:

$$\phi_P = \frac{U}{4\pi\rho g}\iint_{S_P} P(\xi, \eta)G_x(x-\xi; y-\eta; z, 0)d\xi d\eta\ , \qquad (4)$$

after performing an integration by part in $\xi$. The Green function $G$ is given in [3]:

$$\begin{aligned} G(x-\xi; y-\eta; z, \zeta) &= -\frac{1}{r}+\frac{1}{r_1}+\frac{4k_0}{\pi}\int_0^{\pi/2} d\theta\sec^2\theta \\ &\int_0^\infty dk\frac{e^{k(z+\zeta)}}{k-k_0\sec^2\theta}\cos[k(x-\xi)\cos\theta]\cos[k(y-\eta)\sin\theta] \\ &+ 4k_0\int_0^{\pi/2} d\theta\sec^2\theta e^{k_0(z+\zeta)\sec^2\theta}\sin[k_0(x-\xi)\sec\theta] \\ &\times\cos[k_0(y-\eta)\sin\theta\sec^2\theta] \\ &\equiv G_L + G_w \end{aligned} \qquad (5)$$

*Visiting Scholar: Dept. of Naval Arch. & Marine Engrg., Chungnam National University, Taejon 305-764, Korea where $G_L$ and $G_w$ denote the terms that are symmetric (the first three) and asymmetric with respect to $(x-\xi)$, respectively.

The wave resistance induced by a moving cushion is given by the integral of product of the pressure $P$ and free-surface slope Eq. (3): $-\iint_{S_P} P(x,y)\zeta_x d\xi d\eta$ and can be simplified to (with the change of variable $\lambda = \sec\theta$):

$$R_{w_P} = \pi\rho U^2 \int_1^\infty \frac{d\lambda}{\lambda^4\sqrt{\lambda^2-1}} |A_P(\lambda)|^2, \quad (6)$$

where $A_P(\lambda)$, the complex wave-making amplitude (or the Kochin) function, is given by :

$$A_P(\lambda) = \frac{k_0\lambda^4}{\pi\rho U^2} \iint_{S_P} P(\xi,\eta) e^{ik_0\lambda(\xi+\sqrt{\lambda^2-1}\eta)} d\xi d\eta \quad (7)$$

In arriving at Eq. (6), we note that there was no contribution from $G_L$. Further, from Eqs. (6-7), we observe that $R_{wP}$ will be decreased by 75% when pressure $P$ is reduced by 50%. So, smaller $P$ is favored in terms of reducing wave resistance. However this will increase the size of the cushion for a fixed displacement.

A pressure cushion profile of peak value $P_m$ that is infinitely differentiable in the horizontal plane [4] is shown in Fig. 2. This hyperbolic tangent form with the tapering parameters $\alpha$ and $\beta$, in the longitudinal and transverse directions respectively, leads to a closed form expression for (7) (see [2]).

For a confirmation of our computed results with

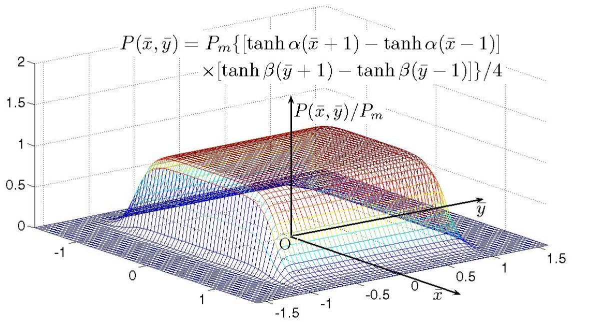


Figure 2: *Pressure function $P(x,y)$ of a cushion ($\alpha$=5, $\beta$=20) in unitized variables: $\overline{x} = 2x/B_p$, $\overline{y} = 2y/L_p$.*

[4], the wave resistance experienced by the pressure cushion is shown in Fig. 3 as a function of the Froude number ($F_n^{-2}$), with the beam-to-length ratio, $B_P/L_P$, of the cushion as a parameter. Here, the non-dimensionalized resistance coefficient is defined by

$$C_{wP} = \frac{R_{wP}}{2P_m^2 B_P/\rho g} \propto \frac{R_{wP}}{2\Delta(h/L_P)}, \quad (8)$$

where $\Delta$ is the displacement (or "lift") due to the cushion, and $h/L_P$ is the (hydrostatic) head of $P_m$ to cushion length $L_P$ ratio. The plot provides the interesting observation: The wave drag to displacement ratio is proportional to the head-to-length ratio times a function that depends only on $B_P/L_P$ and $F_n$. In Fig. 3,for a fixed $h/L_P$, a wide cushion always yields higher resistance. The highly oscillatory behavior is related to the interference of the waves generated by the bow and stern of the cushion.

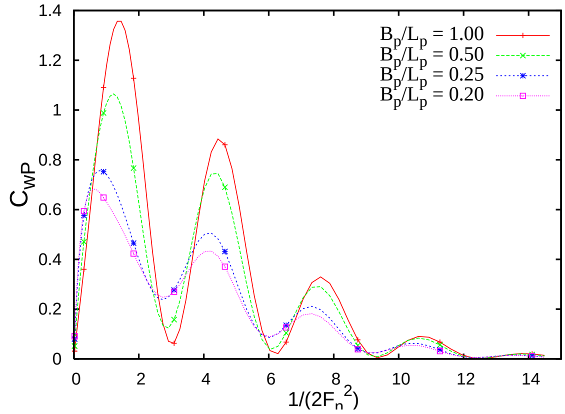


Figure 3: $C_{wP}$ *for a rectangular cushion,* $\alpha$=5, $\beta$=20.

## 3 Dual Cushions with Separation and Stagger

In the case of two pressure cushions with separation and stagger, as defined in Fig. 1, the total wave resistance $R_{w_T}$ on the two pressure cushions is not only the sum of the resistance due to pressure $P_1(x,y)$ (i.e., $R_{w_{P_1}}$) and pressure $P_2$ ($R_{w_{P_2}}$) individually, but also of an interference term $R_{w_{P_1 \rightleftarrows P_2}}$, which cannot be ignored. This term accounts for the effect of pressure 1 on pressure 2 ($R_{w_{P_1\to P_2}}$) as well as the effect of pressure 2 on pressure 1 ($R_{w_{P_1\leftarrow P_2}}$), or effectively, the superposition of the wave-interference effects of each of the surface distribution in the field. Following [1], we can establish:

$$\begin{aligned} R_{w_T} &= R_{w_{P_1}} + R_{w_{P_2}} + R_{w_{P_1\rightleftarrows P_2}} \\ &= R_{w_{P_1}} + R_{w_{P_2}} + R_{w_{P_1\to P_2}} + R_{w_{P_1\leftarrow P_2}} \quad (9) \end{aligned}$$

where $R_{w_{P_1}}$ and $R_{w_{P_2}}$ are each given by the equivalents of the Michell formula [8], or Eq. (6-7) here.

### 3.1 The Interference Resistance $R_{w_{P_1\rightleftarrows P_2}}$

Consider the two local frames of reference, $O_1x_1y_1z_1$ and $O_2x_2y_2z_2$ in Fig.1. Using Eqs. (2-4), we can write the expression of the interference resistances $R_{w_{P_1\to P_2}}$ (pressure 2 acting on the wave slope at cushion 2 generated by cushion 1) and $R_{w_{P_2\to P_1}}$ (pressure 1 acting on the wave slope at cushion 1 generated by cushion 2) as:

$$R_{wP_1\to P_2} = \frac{U^2}{4\pi\rho g^2}\iint_{S_{P_2}} P_2(x_2,y_2)dx_2dy_2\iint_{S_{P_1}} P_1(\xi_1,\eta_1)$$
$$G_{x_2x_2x_2}(x_2+st-\xi_1;y_2+sp-\eta_1;z_2,0)d\xi_1 d\eta_1 \quad (10)$$

$$R_{wP_2\to P_1} = \frac{U^2}{4\pi\rho g^2}\iint_{S_{P_1}} P_1(x_1,y_1)dx_1dy_1\iint_{S_{P_2}} P_2(\xi_2,\eta_2)$$
$$G_{x_1x_1x_1}(x_1-st-\xi_2;y_1-sp-\eta_2;z_1,0)d\xi_2 d\eta_2 \quad (11)$$

Then combining Eqs. (10) and (11), and recalling that $x_2 = x_1 - st,\ y_2 = y_1 - sp$, and $z_2 = z_1$, we can show that the *summed* resistance on the two pressure cushions can be written as:

$$R_{wP_1\rightleftharpoons P_2} = \frac{-U^2}{2\pi\rho g^2}\iint_{S_{P_1}} P_1(x_1,y_1)dx_1dy_1\iint_{S_{P_2}} P_2(\xi_2,\eta_2)$$
$$G_{wx_1x_1x_1}(x_1-st-\xi_2;y_1-sp-\eta_2;0,0)d\xi_2 d\eta_2 \quad (12)$$

Of interest is that only $G_w$ survives in this summation. Eq. (12) is still unwieldy. However, if *both* cushions are symmetric about their own $x$ axis, $P(x,-y) = P(x,y)$, the result simplifies greatly in a manner similar to the hull-to-hull interference problem of [1]. Under this assumption, $A_P$ in Eq. (7) can be written as:

$$A_P(\lambda) = \frac{k_0\lambda^4}{\pi\rho U^2}\iint_{S_P} P(\xi,\eta)e^{ik_0\lambda\xi}\cos(k_0\lambda\sqrt{\lambda^2-1}\eta)d\xi d\eta \quad (13)$$

and the interference resistance is given by:

$$R_{wP_1\rightleftharpoons P_2} = 2\pi\rho U^2\int_1^\infty \frac{d\lambda}{\lambda^4\sqrt{\lambda^2-1}}\cos(k_0 sp\lambda\sqrt{\lambda^2-1})$$
$$\times\{\Re(A_{P_1}\bar{A}_{P_2})\cos(k_0\lambda st) + \Im(A_{P_1}\bar{A}_{P_2})\sin(k_0\lambda st)\} \quad (14)$$

Here, $\Re$ and $\Im$ denote real and imaginary parts, respectively. Similarly, if the pressure cushions have symmetry about the $y$ axis, $P(x,y) = P(-x,y)$, i.e. fore-aft symmetry, then Eq. (7) can be written as:

$$A_P(\lambda) = \frac{k_0\lambda^4}{\pi\rho U^2}\iint_{S_P} P(\xi,\eta)e^{ik_0\lambda\sqrt{\lambda^2-1}\eta}\cos(k_0\lambda\xi)d\xi d\eta, \quad (15)$$

and the interference resistance will be:

$$R_{wP_1\rightleftharpoons P_2} = 2\pi\rho U^2\int_1^\infty \frac{d\lambda}{\lambda^4\sqrt{\lambda^2-1}}\cos(k_0\lambda st)$$
$$\times\{\Re(A_{P_1}\bar{A}_{P_2})\cos(k_0\lambda\sqrt{\lambda^2-1}sp) \quad (16)$$
$$+\Im(A_{P_1}\bar{A}_{P_2})\sin(k_0\lambda\sqrt{\lambda^2-1}sp)\}$$

Eqs. (14) and (16) show explicitly how the staggerand separation between the pressure cushions can influence the total wave resistance. These new expressions can be computed concurrently with the mono-pressure resistances $R_{wj}, j=1,2$, given by Eq. (6).

## 4 Results and Discussion

Restricting the investigation to dual cushions in this paper, we show some sample results of having first dual cushions in parallel, and then in tandem, configurations. For $B_P/L_P = 0.5$, we compare the performance of the dual cushions, each of peak pressure $P_m$, against a mono-cushion of the same displacement and geometry. The mono-cushion resistance $R_0$, therefore, has a pressure of $2P_m$, applied over the same "footprint". Figs. 4 and 5 show the interference and total wave resistance, respectively, relative to $R_0$ for dual cushions in a parallel configuration. In these figures, the surface functions approach unity at $sp = 0$, when the two cushions overlay. Then both functions drop off in an oscillatory manner in both directions. Significant interference drag occurs when $sp/B_p$ is $\sim$ unity and $F_n$ is below the first resistance hollow of the mono-cushion. Note that for large $F_n$ or $sp$, the dual-cushion resistance approaches the expected value of $50\%$ of that of the mono-cushion.

To obtain the actual dual-cushion $C_{wT}$, one should multiply the $R_T/R_0$ ratio by $C_o$, the mono-cushion resistance coefficient defined by Eq. (8), this latter function is plotted as a *trace* against $F_n$ for reference.

The corresponding results of having the dual cushions in tandem with $st$ being varied are shown in Figs. 6 and 7. The oscillatory patterns are more complex. The lower $F_n$ region shows clearly the interefer-ence effects of transverse waves. Besides that, a valley of low total drag occurs for a combination of $F_n$ and $st/L_p$. This valley extends to larger values of $st/L_p$ (partly visible).

The effects of varying both stagger and separation are shown in Figs. 8 and 9 for $F_n = 0.42$, which is at the first hollow, and for a higher Froude number, $F_n{=}1$. Here, $\lambda_o$ is the maximum (transverse) wavelength of the Kelvin wave system. These plots parallel the so-called Weinblum configurations of di-hulls. The behavior at the two speeds are drastically different, but $R_T/R_o$ at $30\%$ is achievable for a wide range of $sp$–$st$ combinations. These and other complex features will be further discussed in the Workshop.

**REFERENCES**


1. Yeung, R.W., Poupard, G. and Toilliez,J.O., *SNAME Trans.*, Vol.112, 2004, pp. 142–169.
2. Yeung, R.W., H. Wan, *ASME J. Offsh Mech & Arctic Engrg*, 2008, in press.
3. Wehausen, J. V. and Laitone, E. V., *Handbuch der Physik*, Vol. 9, Springer-Verlag, Berlin, 1960,
4. Newman,J.N. and Poole, F.A.P., *Shiffstechnik*, Bd. 9, Heft 45, 1962, pp. 21-26.
5. Doctors, L.J. and Sharma, S.D., *J. Ship Res*, Vol. 16, 1972, pp. 248-260
6. Tuck, E. O., Scullen, D.,and Lazauskas, L., *Proc.* $24^{th}$ *Symp. Naval Hydrodyn.* , Fukuoka, Japan, 2002.
7. Burg, Donald E., "Multiple Cushion Air-Ride Boat Hull", WIPO Patent: WO/1992/013753, 1992.
8. Michell, J.H., *Philosophical Magazine*, Ser. 5, Vol. 45, 1898, pp. 106-123.

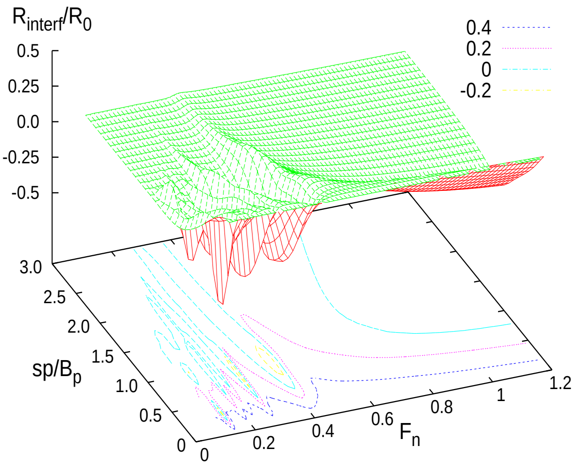


Figure 4: *$R_{interf}/R_0$ for dual cushions vs. $F_n$ and $sp$, for $st = 0$.*

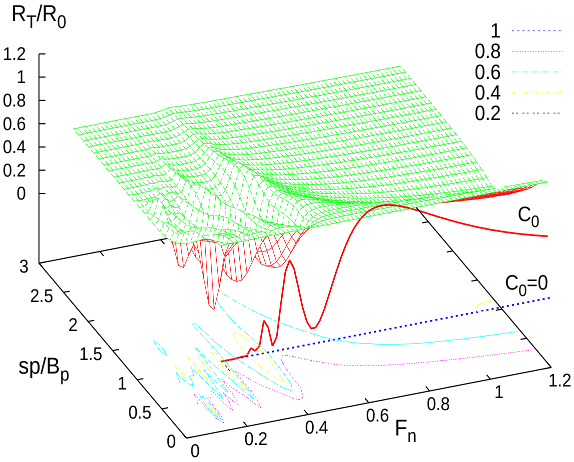


Figure 5: *$R_T/R_0$ vs. $F_n$ and $sp$, for $st = 0$, with $C_0(F_n)$ shown.*

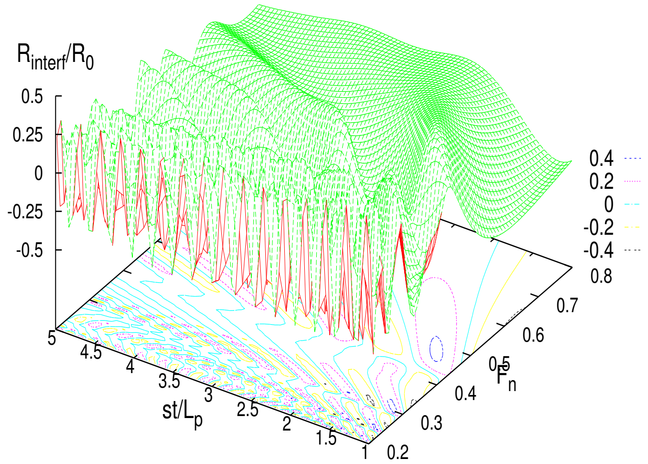


Figure 6: *$R_{interf}/R_0$ vs. $F_n$ and $st$ for dual cushions in tandem $(sp = 0)$.*

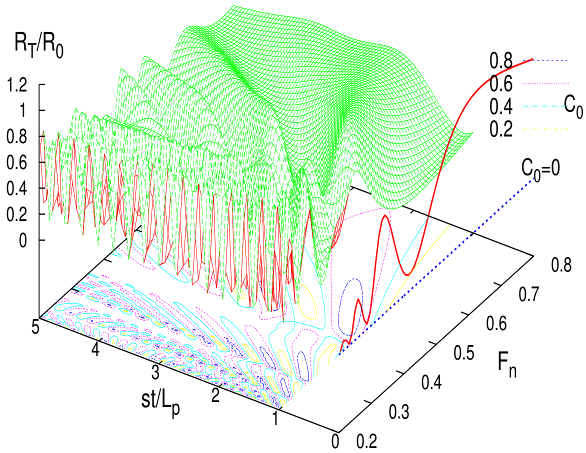


Figure 7: *$R_T/R_0$ vs. $F_n$ and $st$, for dual cushions in tandem $(sp = 0.)$, with $C_0(F_n)$ shown.*

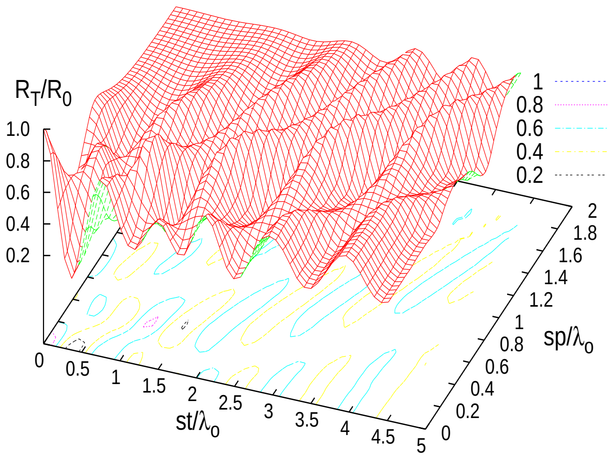


Figure 8: *Dual-cushion $R_T/R_0$ vs. $st/\lambda_o$ and $sp/\lambda_o$, at* $F_n = 0.42$

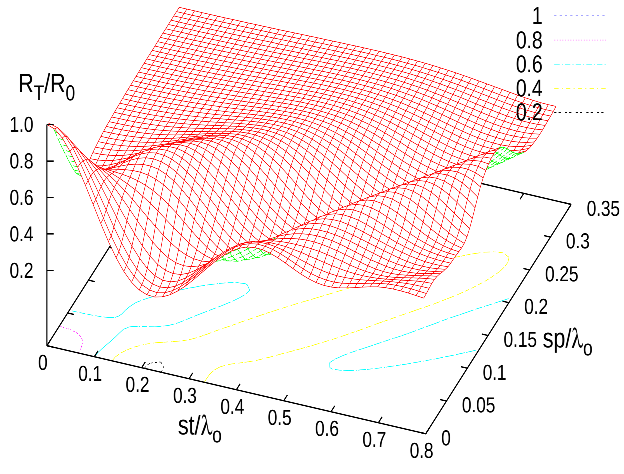


Figure 9: *Dual-cushion $R_T/R_0$ vs. $st/\lambda_o$ and $sp/\lambda_o$, at* $F_n = 1.0$